Article

Computed tomography of the chest with model-based iterative reconstruction using a radiation exposure similar to chest X-ray examination: preliminary observations

NEROLADAKI, Angeliki, *et al*.

Abstract

The purpose of this study was to assess the diagnostic image quality of ultra-low-dose chest computed tomography (ULD-CT) obtained with a radiation dose comparable to chest radiography and reconstructed with filtered back projection (FBP), adaptive statistical iterative reconstruction (ASIR) and model-based iterative reconstruction (MBIR) in comparison with standard dose diagnostic CT (SDD-CT) or low-dose diagnostic CT (LDD-CT) reconstructed with FBP alone.

Reference

NEROLADAKI, Angeliki, *et al*. Computed tomography of the chest with model-based iterative reconstruction using a radiation exposure similar to chest X-ray examination: preliminary observations. *European radiology*, 2013, vol. 23, no. 2, p. 360-6

DOI : 10.1007/s00330-012-2627-7
PMID : 22892722

Eur Radiol (2013) 23:360–366
DOI 10.1007/s00330-012-2627-7

COMPUTED TOMOGRAPHY

Computed tomography of the chest with model-based iterative reconstruction using a radiation exposure similar to chest X-ray examination: preliminary observations

Angeliki Neroladaki · Diomidis Botsikas · Sana Boudabbous · Christoph D. Becker · Xavier Montet

Received: 5 June 2012 / Revised: 18 July 2012 / Accepted: 18 July 2012 / Published online: 15 August 2012

Abstract
Objectives The purpose of this study was to assess the diagnostic image quality of ultra-low-dose chest computed tomography (ULD-CT) obtained with a radiation dose comparable to chest radiography and reconstructed with filtered back projection (FBP), adaptive statistical iterative reconstruction (ASIR) and model-based iterative reconstruction (MBIR) in comparison with standard dose diagnostic CT (SDD-CT) or low-dose diagnostic CT (LDD-CT) reconstructed with FBP alone.
Methods Unenhanced chest CT images of 42 patients acquired with ULD-CT were compared with images obtained with SDD-CT or LDD-CT in the same examination. Noise measurements and image quality, based on conspicuity of chest lesions on all CT data sets were assessed on a five-point scale.
Results The radiation dose of ULD-CT was 0.16±0.006 mSv compared with 11.2±2.7 mSv for SDD-CT ($P<0.0001$) and 2.7±0.9 mSv for LDD-CT. Image quality of ULD-CT increased significantly when using MBIR compared with FBP or ASIR ($P<0.001$). ULD-CT reconstructed with MBIR enabled to detect as many non-calcified pulmonary nodules as seen on SDD-CT or LDD-CT. However, image quality of ULD-CT was clearly inferior for characterisation of ground glass opacities or emphysema.
Conclusion Model-based iterative reconstruction allows detection of pulmonary nodules with ULD-CT with radiation exposure in the range of a posterior to anterior (PA) and lateral chest X-ray.

A. Neroladaki · D. Botsikas · S. Boudabbous · C. D. Becker · X. Montet (✉)
Department of Radiology, Geneva University Hospital, Rue Gabrielle-Perret-Gentil 4, 1211 Geneva 4, Switzerland
e-mail: xavier.montet@hcuge.ch

Key Points
- *Radiation dose is a key concern with the increased use of thoracic CT*
- *Ultra-low-dose chest CT approximates the radiation dose of conventional chest radiography*
- *Ultra-low-dose chest CT can be of diagnostic quality*
- *Solid pulmonary nodules are clearly depicted on ultra-low-dose chest CT*

Keywords Computed tomography · Chest · Low dose · Pulmonary nodules · Model-based iterative reconstruction (MBIR)

Abbreviations

ULD-CT	Ultra-low-dose chest CT
SDD-CT	Standard-dose diagnostic CT
LDD-CT	Low-dose diagnostic CT
FBP	Filtered back projection
ASIR	Adaptive statistical iterative reconstruction
MBIR	Model-based iterative reconstruction
DLP	Dose-length product
CXR	Chest X-ray

Introduction

Computed tomography (CT) is one of the key investigative techniques in diagnostic imaging, and is particularly useful in chest disease. The diagnostic benefit of CT is, however, associated with the inherent risk of ionizing radiation, and its widespread use places CT among the main sources of ionizing radiation in the general population of industrialised countries [1]. On a statistical level, there are concerns that the widespread use of CT might increase the risk of radiation-induced cancer [2].

Major efforts are therefore being made by vendors of CT equipment, radiologists and technicians to minimise the radiation dose of CT examination protocols while maintaining adequate diagnostic image quality. Among the different strategies for radiation-dose reduction, the optimisation of CT hardware like X-ray tube and detectors, the use of X-ray dose modulation [3] and the choice of the most adequate CT examination protocol obviously play a key role. Major progress has also recently been made with regard to the algorithms used for reconstruction of CT images. The traditional method, called filtered back projection (FBP) may now be completed with iterative reconstruction algorithms that intend to decrease the radiation dose while maintaining image quality. The first generation of iterative reconstruction tools, such as adaptive statistical image reconstruction (ASIR) or iterative reconstruction in image space (IRIS) achieve this mainly by decreasing the noise in the reconstructed CT images [4–9]. More recent developments, such as model based iterative reconstruction (MBIR), include an algorithm that accurately models the entire optical chain (real size of focal spot and detectors) and takes into account the noise of the system (photons statistics and electronic noise). As CT data sets reconstructed with an MBIR algorithm have a very low level of noise [10], MBIR carries the potential for even more drastic reduction in dose for obtaining images of diagnostic quality.

The purpose of this study was to investigate whether the use of the MBIR algorithm combined with the latest CT hardware technology allows CT images of the chest of diagnostic quality to be obtained while lowering the radiation dose close to the level of a posterior to anterior (PA) and lateral chest X-ray (CXR).

Materials and methods

Patients

The study was approved by the ethics committee of our hospital. The study included 42 consecutive patients who underwent non-enhanced chest CT between June and August 2011. They were 24 men, aged between 19 and 80 years old, with an average body mass index (BMI) of 25.8 ± 3.9, and 18 women aged between 23 and 70 years old, with an average BMI of 22.8 ± 4.5. CT indications were: follow-up or suspected nodules (n=32), COPD evaluation (n=6), lung transplantation control (n=2) and suspicion of pneumothorax (n=2).

After a first diagnostic CT (either standard-dose diagnostic [SDD] CT or low-dose diagnostic [LDD] CT), a subsequent acquisition was realised at ultra-low-dose (ULD) CT during the same examination. Twenty patients underwent SDD-CT, whereas 22 patients underwent LDD-CT. As LDD-CT equals SDD-CT for lesion detection, they were handled together under the name of diagnostic CT [11, 12].

CT protocols and image reconstruction

All chest CT examinations were acquired using 64-slice multi-detector CT (GE Discovery 750 HD; GE Healthcare, Milwaukee, USA). For SDD-CT acquisition, the usual clinical chest CT protocol was used in helical mode: 0.6-s gantry rotation time, 120 kVp, 0.984:1 beam pitch, 40-mm table feed per gantry rotation, a z-axis tube current modulation was used, with a noise index of 28 (min/max mA, 100/500) and a 64×0.625-mm detector configuration.

For LDD-CT acquisition, the parameters were maintained except that a noise index of 26 (min/max mA, 80/100) was used. Z-axis tube current modulation was still used.

For ultra-low-dose acquisition, all parameters remained unchanged, except that the kVp was lowered to 100 kVp and the tube current was lowered to 10 mA without dose modulation.

SDD-CT and LDD-CT images were reconstructed at 0.625-mm thickness with filtered back projection, whereas ultra-low-dose images were reconstructed at 0.625-mm thickness with filtered back projection, with 40% and 80% adaptive statistical iterative reconstruction (ASIR-40 and ASIR-80, respectively) and with model based iterative reconstruction (MBIR, Veo™ GE Healthcare, Milwaukee, USA).

Assessment of image quality

Objective image noise was calculated using a lung window setting. Regions of interest were drawn inside the trachea immediately over the carina, while carefully avoiding the trachea wall. The mean HU as well as its standard deviation, considered to be noise, were recorded.

Subjective assessment of image quality of all data sets was realised by three radiologists (X.M. with 9 years of experience, D.B. with 7 years of experience, S.B. with 7 years of experience). Images were displayed with a lung window setting (window level, -500; window width, 1,400) and a soft tissue window setting (window level, 40; window width, 350). The images were anonymised, aggregated in folders in a random way and then evaluated by the three readers for their quality.

The radiologists evaluated the normal lung structures (major fissures and small vessels) and bronchi (<2 mm diameter) based on a five-point scale defined as follows:

1 point: Anatomical structures visible at 100% (excellent)
2 points: Anatomical structures visible at > 75% (good)
3 points: Anatomical structures visible between 25% and 75% (fair)

4 points: Anatomical structures visible < 25% (poor)
5 points: Landmarks were not visible at all (unacceptable)

Diagnostic findings

Radiologists were also asked to record any abnormal structures seen in each pulmonary lobe. Abnormal structures were defined following the glossary of terms for thoracic imaging from the Fleischner Society [13]. The number of micro-nodules (≤ 3 mm in size) was recorded. If the number of micro-nodules was fewer than 5, their number was noted, if the number of micro-nodules was more than 5, > 5 (without exact number) was noted. The size of any nodules (> 3 mm) was noted. The presence of ground glass opacity, consolidation, emphysema or bronchiectasis was also noted. Finally, the presence of pleural and pericardial effusion, as well as the presence of mediastinal adenopathy, was noted. Abnormal structures were described on a five-point scale:

1 point: Abnormal structures clearly visible with good demarcation
2 points: Structures visible with blurring but without restriction for diagnosis
3 points: Abnormal structures visible, with blurring and uncertainties about the evaluation
4 points: Abnormal structures barely visible with unreliable interpretation
5 points: Abnormal structures not seen

Radiation dose assessment

To assess the radiation dose associated with the chest CT, the total dose-length product (DLP) was recorded. The effective dose was retrospectively calculated by multiplying the DLP by a factor of 0.020 [14].

Statistical analysis

Statistical analysis was performed with Prism (Prism, version 5d, 2010; GraphPad Software, San Diego, CA, USA) and Statistica (version 8; Statsoft, Tulsa, OK, USA). Inter-observer agreement was performed with R using the kappa fleiss function (R package version 0.83, using the irr library). For ordinal values, the results are presented as median. For continuous values, the results are presented as mean ± standard error.

Non-normally distributed data sets (established from Kolmogorov-Smirnov tests) were compared using Friedman test with Dunn post-hoc test. Normally distributed data sets were compared using ANOVA test with Bonferroni post-hoc test. Two-sided testing was used. Differences were considered significant at $P<0.05$.

Results

Technical parameters

All ULD CTs were reconstructed with FBP, ASIR and MBIR without technical problems. Whereas the FBP and ASIR reconstructions only took a few seconds, about 1-h reconstruction time was needed for the MBIR algorithm.

The dose-length product (DLP) associated with SDD-CT and LDD-CT (diagnostic CT) and ULD CT was 560 ± 138, 133 ± 43 and 8 ± 0.3 mGy·cm, respectively ($P<0.0001$). Estimated effective doses were 11.2 ± 2.7, 2.7 ± 0.9 and 0.16 ± 0.006 mSv for the SDD-CT, LDD-CT and ULD-CT, respectively.

Image quality

The noise of the SDD-CT and LDD-CT were 24 ± 9 and 28 ± 9 HU, respectively. The noise of the ULD-CT was 107 ± 7, 94 ± 5, 77 ± 4 and 23 ± 4 for FBP, ASIR-40, ASIR-80 and MBIR, respectively. The noise of the ULD-CT was statistically higher than the noise on the diagnostic CT using the FBP, and ASIR algorithms ($P<0.0001$), whereas it was not different when using the MBIR algorithm ($P=0.76$). The BMI did not influence the image quality/noise of the image.

The subjective image quality assessment for the three readers is summarised in Tables 1 and 2. The normal lung structures on diagnostic CT (either SDD-CT or LDD-CT)

Table 1 Conspicuity of all the fissures

Fissure		Median R1	R2	R3	*P*
Diagnostic CT (SDD/LDD)		1	1	1	n.s.
ULD-CT	FBP	3*	3*	3*	n.s.
	ASIR-40	3*	3*	3*	n.s.
	ASIR-80	3*	3*	2*	n.s.
	MBIR	2*	2*	2*	n.s.
Diagnostic CT vs ULD-CT		*$P < 0.001$	*$P < 0.001$	*$P < 0.001$	

ULD ultra-low dose, *FBP* filtered back projection, *ASIR* adaptive statistical iterative reconstruction, *MBIR* model-based iterative reconstruction, *n.s.* not significant

Table 2 Conspicuity of the small peripheral artery and bronchi

Anatomy		Median R1	R2	R3	*P*
Diagnostic CT (SDD/LDD)		1	1	1	ns
ULD-CT	FBP	4*	3*	3*	<0.01
	ASIR-40	3*	3*	3*	n.s.
	ASIR-80	2*	2*	2*	n.s.
	MBIR	2*	2*	2*	n.s.
Diagnostic CT vs ULD-CT		*$P < 0.001$	*$P < 0.001$	*$P < 0.001$	

were of high quality with a median value of 1. When acquired with the ultra-low-dose techniques, the quality of the chest CT increased from FBP to ASIR to MBIR. This increased quality was statistically significant for the three readers on each reconstruction algorithms ($P<0.001$). Increased image quality is demonstrated in Fig. 1.

Diagnostic findings

The number of solid nodules (> 3 mm) seen on each data set is summarised in Table 3. There was no statistical difference between the numbers of nodules seen by the readers, nor between the different reconstruction algorithms. Based on the diagnostic CT, 28 nodules of 5.8 ± 3.2 mm were depicted by reader one, 29 nodules of 5.9 ± 2.6 mm were depicted by reader 2 and 29 nodules of 5.7 ± 3.1 mm by reader 3. The inter-observer agreement was almost perfect for the diagnostic CT and for the MBIR algorithm (kappa value of 0.815 for both), whereas it was substantial for FBP and ASIR-80 and moderate for ASIR-40. An example of nodules seen on diagnostic CT and on ULD-CT is presented in Fig. 2. The sensitivity of nodule detection on ULD-CT compared with SDD-CT was 100% for all readers.

The number of micro-nodules (≤ 3 mm) seen on each reconstruction algorithm is summarised in Table 4. The number of micro-nodules seen by each reader on each reconstruction algorithm was not statistically different. When acquired with the ULD techniques, the number of

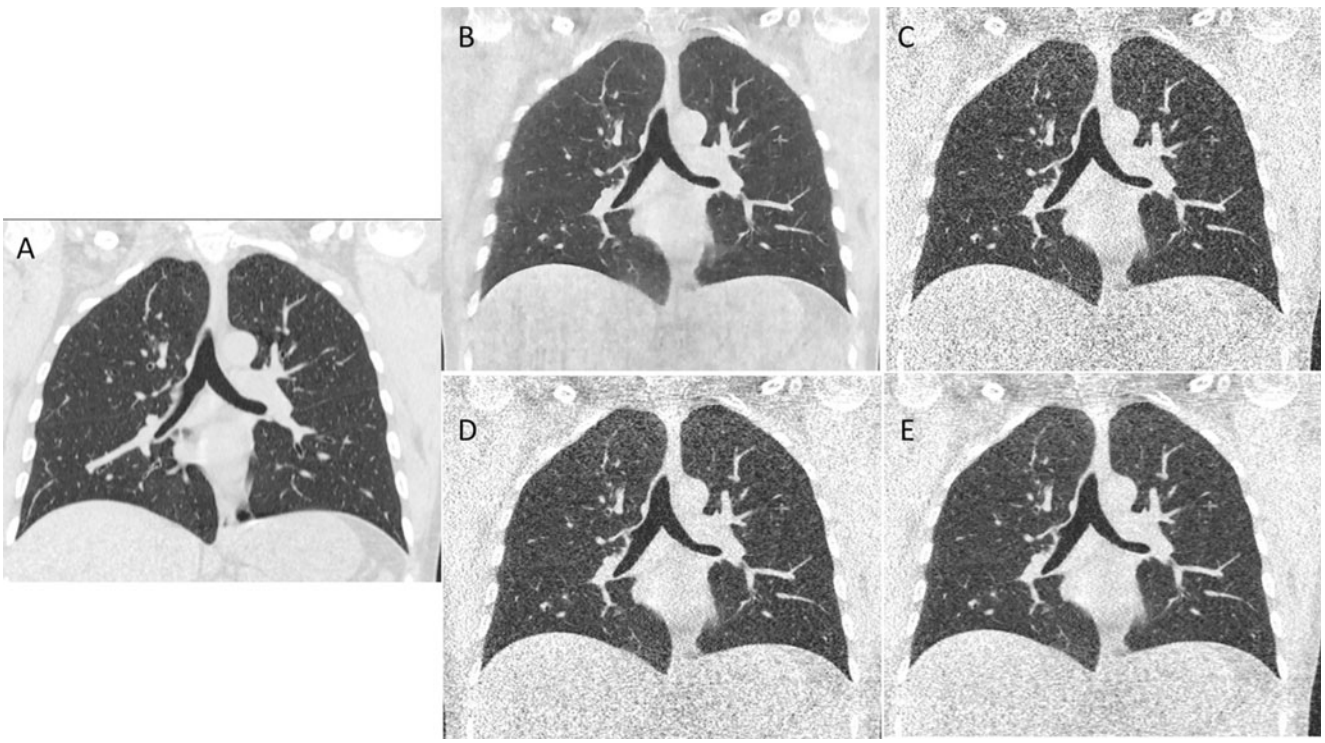

Fig. 1 Image quality. Coronal reformatted CT demonstrating the image quality of a diagnostic CT (**a**). The same patient is presented after an ultra-low-dose acquisition, reconstructed with a MBIR (**b**), FBP (**c**), ASIR-40 (**d**) and ASIR-80 (**e**) algorithms. There was a clear reduction in noise in the image when iterative reconstructions were used, as well as a clear increase in image quality. The MBIR algorithm achieved the highest subjective image quality among the algorithms used to reconstruct ULD CT (see Tables 1 and 2)

Table 3 Number of nodules

Nodules		Number of nodules R1	R2	R3	Kappa
Diagnostic CT (SDD/LDD)		28	29	29	0.815
ULD-CT	FBP	25	24	19	0.684
	ASIR-40	27	28	18	0.578
	ASIR-80	28	29	20	0.654
	MBIR	28	29	29	0.815
Diagnostic CT vs ULD-CT		n.s.	n.s.	n.s.	

Table 4 Number of micro-nodules

Micro-nodules		Number of micro-nodules R1	R2	R3	Kappa
Diagnostic CT (SDD/LDD)		137	117	126	0.298
ULD-CT	FBP	71*	71	75	0.476
	ASIR-40	85	86	82	0.386
	ASIR-80	98	94	89	0.855
	MBIR	147	130	111	0.551
Diagnostic CT vs ULD-CT		*$P < 0.05$	ns	ns	

micro-nodules seen increased from FBP to ASIR to MBIR, without reaching a statistical difference. The only statistical difference was noted for the FBP techniques for reader 1, which depicted fewer micro-nodules than all other reconstruction techniques. Nevertheless, the trend to depict more micro-nodules when adding some iterative reconstruction was clear. The sensitivity of ULD-CT for the detection of micro-nodules (compared with SDD-CT) was 107%, 111% and 88% for reader 1,2 and 3, respectively.

Bronchiectasis and architectural distortion were described with a perfect agreement between the readers on the diagnostic CT as well as the ULD-CT, when reconstructed with MBIR.

The number of patients having ground-glass opacities is summarised in Table 5. GGO was described on 11 (readers 1 and 2) and 12 (reader3) patients on the diagnostic CT corresponding to a substantial agreement. The inter-observer agreement was slight for the FBP and ASIR-40 data set and was fair for the ASIR-80 and MBIR data set.

The number of patients having emphysema seen on each data set is summarised in Table 6. Emphysema was diagnosed in nine patients by all readers on the diagnostic CT (perfect agreement). There was almost no agreement between the readers on all the ULD data sets (kappa values between -0.317 and 0.06).

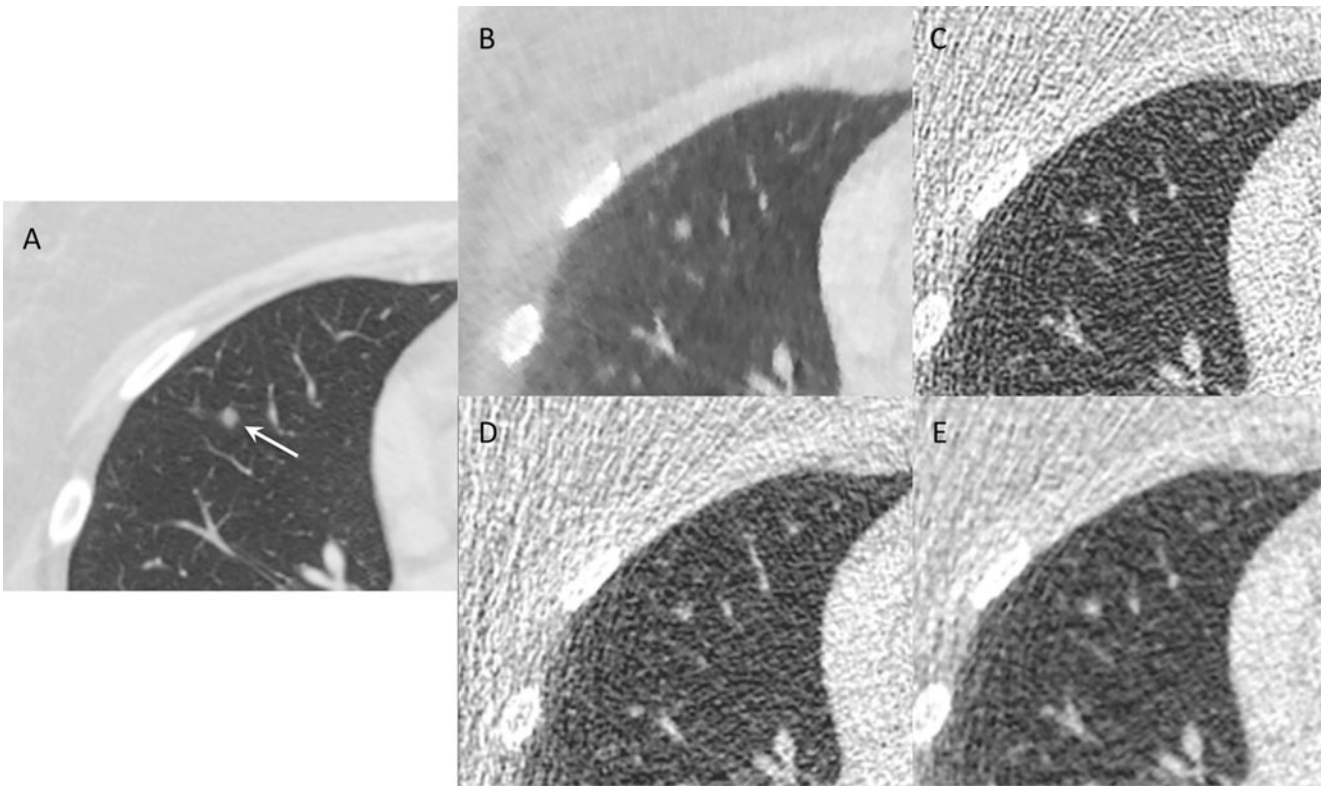

Fig. 2 Nodules. Diagnostic CT showing a 5-mm nodule (*arrow*) in the right middle lobe (**a**). The same nodule seen on ULD-CT, reconstructed with MBIR (**b**), FBP (**c**), ASIR-40 (**d**) and ASIR-80 (**e**) algorithms

Table 5 Number of patients having ground glass opacities

GGO		Kappa	Five-point scale (median)	Number of patients R1	R2	R3
Diagnostic CT (SDD/LDD)		0.694	1	11	11	12
ULD-CT	FBP	0.172	2	7	11	9
	ASIR-40	0.222	1.5	9	10	8
	ASIR-80	0.184	1	9	9	8
	MBIR	0.367	1	8	14	11

Pleural, pericardial effusions and lymph nodes were described by all readers on SDD-CT and LDD-CT and MBIR data sets. Some subtle pericardial effusions were missed on the ULD-CT reconstructed with FBP or ASIR algorithms.

Discussion

Despite all the technological developments in CT, the reconstruction algorithm, namely FBP, has remained unchanged since the 1970s. Although FBP allows very rapid image reconstruction, this algorithm suffers from major drawbacks due to approximation of the real focal spot and detector sizes, and the data are corrupted by quantum and electronic noise during the acquisition, thus propagating image noise [15].

The first generation of iterative reconstruction, including ASIR or IRIS, takes into account how noise propagates during the reconstruction steps and feeds this information back into the loop to iteratively reduce noise in the reconstructed image. Recent clinical data have shown that iterative reconstructions with IRIS using three iterations provide similar image quality to chest CT with 35% less dose compared with FBP reconstruction [6]. When using ASIR, hybrid reconstruction algorithms combining FBP and ASIR at varying percentages allow iterative reconstructions to be adapted to different diagnostic settings; ASIR-40 and ASIR-80 were used arbitrarily in our study protocol, and the data were listed separately.

Table 6 Number of patients having emphysema

Emphysema		Kappa	Five-point scale (median)	Number of patients R1	R2	R3
Diagnostic CT (SDD/LDD)		1	1	9	9	9
ULD-CT	FBP	0.06	2	5	6	5
	ASIR-40	−0.125	1.5	4	5	3
	ASIR-80	−0.317	1	8	5	6
	MBIR	−0.144	2.2	11	16	6

The second generation of iterative reconstruction algorithms, including MBIR, accurately models the production of X-rays in the tube and the attenuation of these X-rays within the patient and the CT system. MBIR also models the measurements inside the detectors and the transformation into the digital signal. All these models are fed into a mathematical model to describe the reconstructed image in a manner representative of the projection data. The resulting function is optimised to find the best possible match between the reconstructed image and the acquired projection data. Hence, this system minimises discrepancies between the projection data and the theoretical model. Our results regarding image quality demonstrate that the use of MBIR offers even further reduction of noise compared with ASIR alone. Noise reduction of 12%, 28% and 79% was achieved for ASIR-40, ASIR-80 and MBIR, respectively, which is in agreement with recently reported results of other investigators [16].

Clinical evaluation of the potential of dose reduction in chest CT may be done by using variations of different technical parameters that may influence image quality; namely, kilovoltage, tube current and reconstruction algorithms. The use of MBIR holds promise to allow even more drastic dose reduction in chest CT compared with ASIR. We designed to investigate the diagnostic value of chest CT reconstructed with ASIR-40, ASIR-80 and MBIR with a radiation dose close to a PA and lateral CXR, in comparison with SDD-CT or LDD- CT.

Our ULD- CT protocol resulted in an exposure of 0.16 ± 0.006 mSv, close to the dose of a PA and lateral CXR, which is reported between 0.05 and 0.24 mSv in the literature [17–21]. This corresponds to a dose reduction of 98.6% compared with SDD-CT and 94% compared with LDD-CT.

An increase in subjective image quality with the use of ASIR and even more with the use of MBIR, seems to translate into a higher inter-observer agreement regarding dense lesions encountered in the lung parenchyma. Nevertheless, a unique image feature of MBIR data sets (a pixellated blotchy appearance, as already described [16]) was clearly seen in this study, but had little effect on diagnostic quality. Despite anonymisation, MBIR data sets were recognised by the readers.

Results of our study suggest that ULD-CT may enable the detection of pulmonary nodules with a similar sensitivity as SDD-CT or LDD-CT. This could perhaps be taken into consideration in the context of screening protocols focusing specifically on the detection of pulmonary nodules, since radiation exposure plays a key role in image-based screening protocols [22].

Since most of our patients had normal BMI (25 for male and 22 for female patients), additional data are needed to assess image quality of patients with high BMI (BMI>25).

Some drawbacks of the ULD-CT protocol used in our study must, however, be considered. We found that ULD-CT was less adequate for the detection of diagnostic elements of chronic lung disease. Although bronchiectasis was equally well detected as with SDD-CT or LDD-CT, this was not the case for ground-glass opacities and emphysema. Additional studies therefore appear necessary to optimise the image quality in order to detect these diagnostic elements reliably. Implementation of MBIR results in much longer image reconstruction time, requiring an hour or more. In clinical practice, this certainly appears as a drawback in emergency settings, although it may be acceptable in routine indications, such as chronic lung disease, oncological follow-up or screening for lung disease. Nevertheless, due to the constant increase of computing power, one may speculate that in the next few years, the MBIR reconstruction may only take a few seconds.

Finally, we are unable to explain the fact that more micronodules were identified on the MBIR data set than on SDD-CT with FBP. Since the spatial resolution increases with the use of MBIR [23], this could possibly lead to better conspicuity of micro-nodules on the MBIR data set compared with SDD-CT with back projection, regardless of the reduction in X-ray dose. Since histopathological correlation with the radiological findings was not available it is impossible to exclude false-positive results, i.e. that ULD-CT reconstructed with MBIR algorithm could have shown micronodules that did not exist.

In summary, our preliminary data suggest that ULD-CT of the chest acquired with an X-ray dose of a conventional radiography and the MBIR reconstruction algorithm enables detection of non-calcified solid nodules and micro-nodules with similar sensitivity compared with SDD-CT or LDD-CT using FBP. This could perhaps be considered when designing future screening protocols focusing on the detection of solid pulmonary nodules. The detection of subsolid nodules will require additional study, as none were present in this study.

References

1. Brenner DJ, Hall EJ (2007) Computed tomography—an increasing source of radiation exposure. N Engl J Med 357:2277–2284
2. Brenner DJ (2004) Radiation risks potentially associated with low-dose CT screening of adult smokers for lung cancer. Radiology 231:440–445
3. Lee S, Yoon SW, Yoo SM et al (2011) Comparison of image quality and radiation dose between combined automatic tube current modulation and fixed tube current technique in CT of abdomen and pelvis. Acta Radiol 52:1101–1106
4. Leipsic J, Nguyen G, Brown J, Sin D, Mayo JR (2010) A prospective evaluation of dose reduction and image quality in chest CT using adaptive statistical iterative reconstruction. AJR Am J Roentgenol 195:1095–1099
5. Pontana F, Duhamel A, Pagniez J et al (2011) Chest computed tomography using iterative reconstruction vs filtered back projection (Part 2): image quality of low-dose CT examinations in 80 patients. Eur Radiol 21:636–643
6. Pontana F, Pagniez J, Flohr T et al (2011) Chest computed tomography using iterative reconstruction vs filtered back projection (Part 1): evaluation of image noise reduction in 32 patients. Eur Radiol 21:627–635
7. Prakash P, Kalra MK, Digumarthy SR et al (2010) Radiation dose reduction with chest computed tomography using adaptive statistical iterative reconstruction technique: initial experience. J Comput Assist Tomogr 34:40–45
8. Sato J, Akahane M, Inano S, et al. (2011) Effect of radiation dose and adaptive statistical iterative reconstruction on image quality of pulmonary computed tomography. Jpn J Radiol
9. Singh S, Kalra MK, Gilman MD et al (2011) Adaptive statistical iterative reconstruction technique for radiation dose reduction in chest CT: a pilot study. Radiology 259:565–573
10. Scheffel H, Stolzmann P, Schlett CL, et al. (2011) Coronary artery plaques: Cardiac CT with model-based and adaptive-statistical iterative reconstruction technique. Eur J Radiol
11. Bankier AA, Schaefer-Prokop C, De Maertelaer V et al (2007) Air trapping: comparison of standard-dose and simulated low-dose thin-section CT techniques. Radiology 242:898–906
12. Muangman N, Maitreesorrasan N, Totanarungroj K (2011) Comparison of low dose and standard dose MDCT in detection of metastatic pulmonary nodules. J Med Assoc Thai 94:215–223
13. Hansell DM, Bankier AA, MacMahon H, McLoud TC, Muller NL, Remy J (2008) Fleischner Society: glossary of terms for thoracic imaging. Radiology 246:697–722
14. Huda W, Magill D, He W (2011) CT effective dose per dose length product using ICRP 103 weighting factors. Med Phys 38:1261–1265
15. Pan X, Sidky EY, Vannier M (2009) Why do commercial CT scanners still employ traditional, filtered back-projection for image reconstruction? Inverse Probl 25:1230009
16. Katsura M, Matsuda I, Akahane M et al (2012) Model-based iterative reconstruction technique for radiation dose reduction in chest CT: comparison with the adaptive statistical iterative reconstruction technique. Eur Radiol 22:1613-1623
17. Bacher K, Smeets P, Bonnarens K, De Hauwere A, Verstraete K, Thierens H (2003) Dose reduction in patients undergoing chest imaging: digital amorphous silicon flat-panel detector radiography versus conventional film-screen radiography and phosphor-based computed radiography. AJR Am J Roentgenol 181:923–929
18. Mettler FA Jr, Huda W, Yoshizumi TT, Mahesh M (2008) Effective doses in radiology and diagnostic nuclear medicine: a catalog. Radiology 248:254–263
19. Quaia E, Baratella E, Cernic S et al (2012) Analysis of the impact of digital tomosynthesis on the radiological investigation of patients with suspected pulmonary lesions on chest radiography. Eur Radiol. doi:10.1007/s00330-012-2440-3
20. Samara ET, Aroua A, Bochud FO et al (2012) Exposure of the Swiss population by medical x-rays: 2008 review. Health Phys 102:263–270
21. Schuncke A, Neitzel U (2005) Retrospective patient dose analysis of a digital radiography system in routine clinical use. Radiat Prot Dosimetry 114:131–134
22. Saghir Z, Dirksen A, Ashraf H et al (2012) CT screening for lung cancer brings forward early disease. The randomised Danish Lung Cancer Screening Trial: status after five annual screening rounds with low-dose CT. Thorax 67:296–301
23. Yu Z, Thibault JB, Bouman CA, Sauer KD, Hsieh J (2011) Fast model-based X-ray CT reconstruction using spatially nonhomogeneous ICD optimization. IEEE Trans Image Process 20:161–175